

## Failure analysis of a Ti-6Al-4V ultrasonic horn used in cavitation erosion tests

D. Nedelcu, V. Cojocar, M. Nedeloni, F. Peris-Bendu, A. Ghican

"Efimie Murgu" University of Resita, Department of Mechanics and Materials Engineering, Traian Vuia Sq., no.1-4, 320085 Resita, Romania, E-mail: d.nedelcu@uem.ro

 <http://dx.doi.org/10.5755/j01.mech.21.3.10023>

### 1. Introduction

The cavitation erosion behavior of metallic materials is investigated in laboratory conditions through tests performed on various facilities: vibratory apparatus, high-pressure water jet systems, cavitation tunnels, rotating disk devices. The vibratory method is most commonly used because of the lower working time compared to the time from the other methods [1]. This method presents two configurations of specimen set-ups: specimen attached to the vibratory ultrasonic horn ("direct method") and stationary specimen, which is not attached to the ultrasonic horn ("indirect method").

In the direct vibratory method (standardized by ASTM G 32-06 [2]), an oscillation of high frequency and low amplitude is generated by an electro-acoustic converter (piezoelectric crystal) powered by an ultrasonic generator. The oscillation is transmitted by a mechanical transducer (booster) to an ultrasonic horn (also called "sonotrode"). The specimen is attached on the tip of the ultrasonic horn (Fig. 1, according to [2]). The system is designed and calibrated to obtain an oscillation at a frequency of  $f = 20$  kHz and at an amplitude of  $A = 50$  micrometers (peak to peak) on the specimen test surface (front end surface of the specimen). The specimen is immersed in the liquid (usually distilled water). The oscillation generates air cavities in the liquid volume which collapse when coming into contact with the specimen surface, generating cavitation erosion pitting.

The indirect vibratory method introduces a change in the placement of the specimen. It is no longer attached to the ultrasonic horn. Instead it is disposed at a distance of 0.5-1 mm from its tip. This change simplifies the geometry of the ultrasonic horn and of the specimen but generates considerably higher testing times. The literature mainly indicates the use of this testing configuration [3-5], but on materials with high resistance to cavitation erosion (e.g. the materials used in hydraulic turbines components) the testing times can reach 3000-4000 minutes, ten times higher compared to the direct method [3, 6, 7].

The mechanical connections between the components of the ultrasonic system shown in Fig. 1, are made by threaded joints. The joint between the specimen and the ultrasonic horn (only used to direct vibratory method) is subject to the phenomenon of fatigue. It is positioned close to the surface with the maximum amplitude oscillation (the end of the specimen).

The literature indicates a lifetime for ultrasonic horns, working at frequencies of 20 kHz, of around  $10^{12}$  cycles [8, 9]. Practical experience in using these testing systems showed the occurrence of cracks in the ultrasonic

horn thread, after a number of cycles, and working times smaller than expected. On the ultrasonic horn shown in Fig. 2, made of Ti-6Al-4V, the failure occurs after about 15 hours of tests ( $10^9$  cycles, at a frequency of 20 kHz). This behavior was repeated on two ultrasonic horns. All of them have the external thread M12x1, used for the specimen clamping.

The occurrence of a crack on the ultrasonic horn or on the specimen, causes the modification of the resonance frequency of the vibratory system (piezoelectric crystal - booster - ultrasonic horn - specimen), that may go out of range of the generator's working frequencies. The process of according in frequency imposed by the generator causes the rapid propagation of the crack and the occurrence of a fracture. The life of an ultrasonic horn is thus calculated up to the initiation of a crack. On the ultrasonic horn shown in Fig. 2, the fatigue crack propagated on approximately 50% of the thread cross - section.

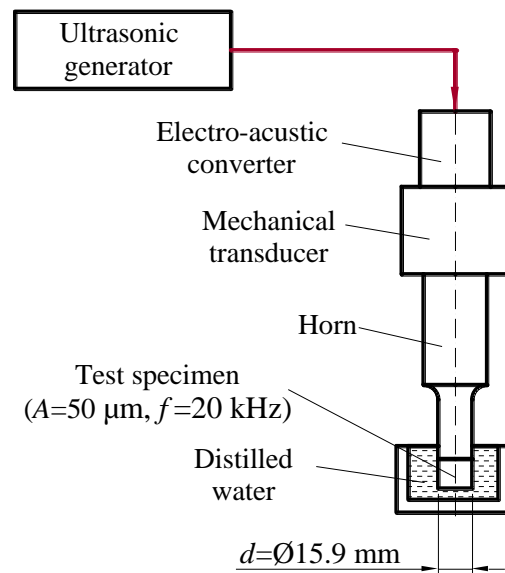


Fig. 1 Equipment set-up on cavitation erosion tests by direct vibratory method

One factor that can lead to the occurrence of micro-cracks and stress concentration areas is the repeated attaching and detaching of the test specimen to the horn. The test procedure involves the weighing of the specimen at regular intervals of time (usually 15 minutes). The preload applied by thread must be made so as to ensure the transmission of oscillation. The analysis of safety factors obtained from static and fatigue analysis must be correlated with this observation.

The paper presents an analysis of the stress state that arises on the ultrasonic horn during cavitation erosion tests and an estimation of the lifetime. Four geometries of horns were analyzed: the original horn with external thread M12x1 and three horns with optimized geometry with internal thread M12x1, M10x1 and M8x1.

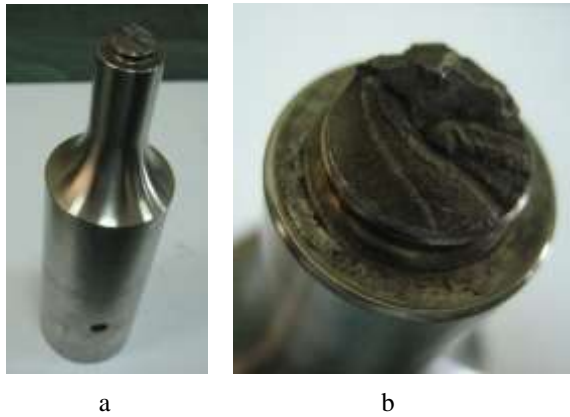


Fig. 2 Ultrasonic horn with fractured thread

## 2. Analysis configuration

The analysis of stress distribution and fatigue life was conducted on the four geometries of the ultrasonic horn, which are codified as UH1, UH2, UH3 and UH4 (Table 1). The four ultrasonic horns have the same main dimensions; the differences are represented by the type and the dimensions of the thread from the horn – test specimen connection.

Table 1  
Configuration of ultrasonic horns

Code	Thread type	Thread dimensions
UH1	external	M12x1
UH2	internal	M12x1
UH3	internal	M10x1
UH4	internal	M8x1

Ultrasonic horn UH1 has the original geometry where failure occurred. The modifications adopted for UH2, UH3 and UH4 geometries were chosen so as to increase the cross sectional area of the threaded area. The nominal dimensions of the threads were chosen in correlation with the outer diameter of the test specimen,  $d = 15.9$  mm, imposed by the ASTM G32 standard (the end diameter of the ultrasonic horn must be equal or close to the diameter of the specimen to avoid the occurrence of cavitation bubbles in the area of interface between the two elements). Fig. 3 shows details of the thread area of the four geometries that were analyzed.

The modifications imposed to UH2, UH3 and UH4 do not change the parameters of the oscillation. Numerical simulations and experimental researches, according to the procedure described in [10], were performed to verify the resonance frequency of the system booster – ultrasonic horn – test specimen.

The material used for UH1-UH4 was Ti-6Al-4V, solution treated and aged, with mechanical properties that are shown in Table 2 [11]. The simulations were made assuming the linear elastic and isotropic behavior of the material.

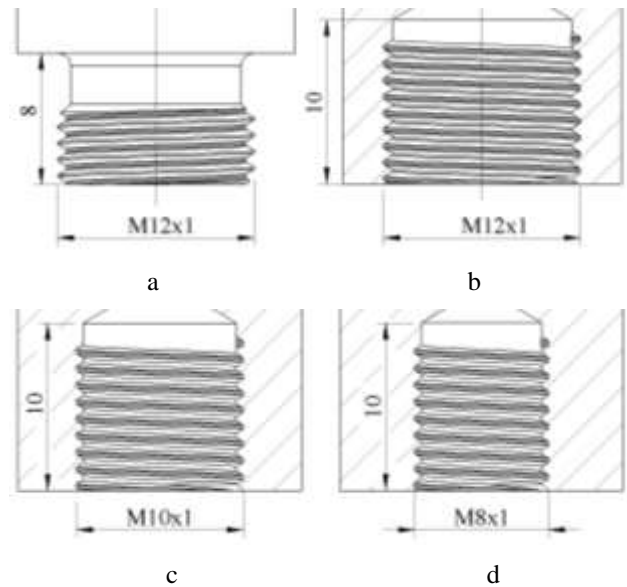


Fig. 3 Details on threaded area of ultrasonic horns: a - UH1; b - UH2; c - UH3; d - UH4

Table 2  
Mechanical characteristics of Ti-6Al-4V [11]

Material	Ti-6Al-4V (SS)
Tensile strength, $R_m$ , N/mm <sup>2</sup>	1050
Yield strength, $R_y$ , N/mm <sup>2</sup>	827
Elastic modulus, $E$ , N/mm <sup>2</sup>	104800
Shear modulus, $G$ , N/mm <sup>2</sup>	41023.8
Poisson's ratio:	0.31

Static FEM simulations were done for each of the four ultrasonic horns with the aim to determine the equivalent von Mises stress distribution. Fatigue analysis was conducted based on the stress state obtained from static studies. Both types of simulations were performed using the SolidWorks software.

The following boundary conditions were applied in the static analysis (Fig. 4):

- Fixing of the horn's front surface (zero degrees of freedom), which is in contact with booster;
- Axial displacement,  $Z = 0.05$  mm (oscillation amplitude) at the end of the ultrasonic horn's threaded area.

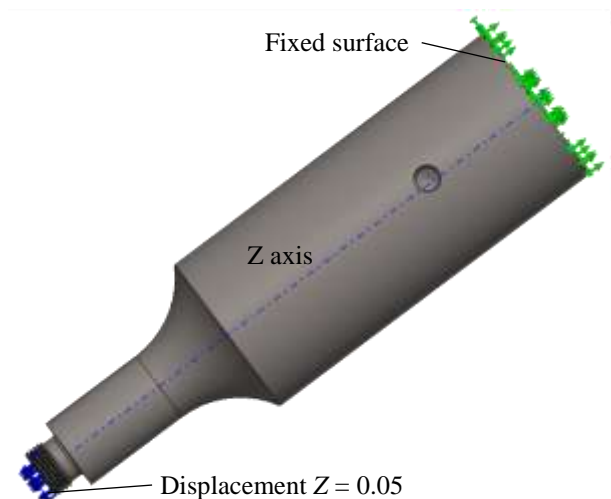


Fig. 4 The restrictions applied to the ultrasonic horn

On the meshing of the models, three zones were

defined, depending on the finite elements' sizes (Fig. 5):

- Zone A (the main cylindrical area) where a curvature based mesh using tetrahedral finite elements with a 4 mm maximum size and a 0.8 mm minimum size was applied;
- Zone B (the horn radius and the cylindrical area with a reduced diameter) where a local mesh using finite elements with a maximum size: 2 mm (case 1), 1 mm (case 2) and 0.8 mm (case 3) with a maximum distortion ratio  $R = 1.5$  was applied. The three cases were defined in order to study the mesh convergence;
- Zone C (threaded area) where a local mesh using finite elements with a maximum size of 0.4 mm and a maximum distortion ratio  $R = 1.5$  was applied.

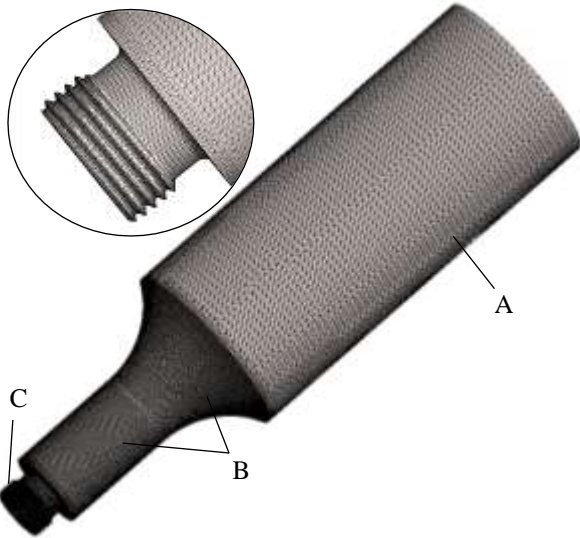


Fig. 5 Mesh applied to the ultrasonic horn

Table 3 summarizes the properties of the mesh (the number of finite elements and the number of nodes) which correspond to the four horns and the three cases that were analyzed. One can observe that the number of finite elements used for case 3 is 3-4 times higher than the number of finite elements used for case 1.

Table 3

Mesh parameters

Code	Parameter	Case 1	Case 2	Case 3
UH1	Elements	152074	207807	459774
	Nodes	219948	298874	652760
UH2	Elements	102658	176727	497349
	Nodes	159507	269949	741628
UH3	Elements	92252	158874	449544
	Nodes	141099	239854	662591
UH4	Elements	84233	144123	393376
	Nodes	127277	215333	575740

Fatigue behavior simulations were performed in order to estimate the life of the horn. In these simulations the maximum stress which arise in static analysis was introduced and the alternating load cycles with  $R = -1$  were defined.

The S-N curves for Ti-6Al-4V (the variation of the alternating stress -  $S$ , depending on the number of fatigue cycles -  $N$ ), were drawn in the literature for up to  $10^7$ - $10^8$  cycles [12, 13]. A small decrease of stress or a constant evolution is considered for a higher number of cycles [14, 15]. The S-N curve used in simulations (Fig. 5)

was adopted from the SolidWorks library. Because the study aimed to analyze the fatigue behavior for a life of  $10^{10}$ - $10^{12}$  cycles, the minimum value of the stress from the S-N curve ( $537.8 \text{ N/mm}^2$ ) was used in the fatigue safety factor estimation.

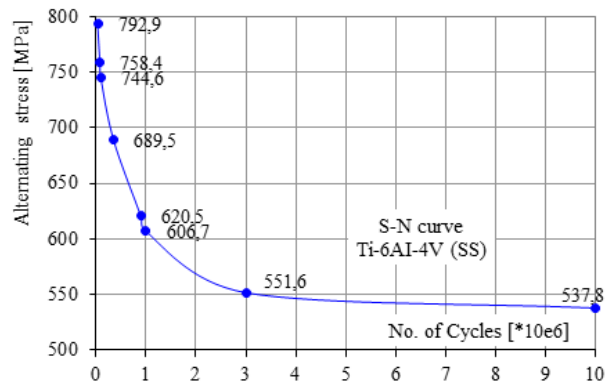


Fig. 6 S-N curve for Ti-6Al-4V, solution treated and aged [11]

### 3. Results

Static simulations show distribution of equivalent von Mises stress on UH1 with high values located in the area of the thread (Fig. 7). For the other areas of the part, the stress was up to  $50$ - $100 \text{ N/mm}^2$ , values which are considered adequate in relation to the mechanical characteristics of the material. The analysis was focused only on the thread area. The maximum stress obtained at HS1 – HS4 for the three cases of mesh are shown in Table 4. Detailed analysis and simulation of the fatigue behavior was performed for the stress corresponding to the mesh with the highest number of finite elements (case 3).

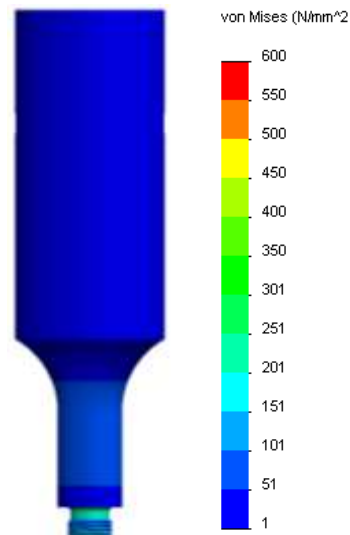


Fig. 7 Von Mises stress distribution in UH1 horn

Table 4

Maximum von Mises stress

Simulation case	Maximum equivalent stress $\sigma_{Von Mises}, \text{ N/mm}^2$			
	UH1	UH2	UH3	UH4
Case 1	588.0	501.9	394.4	350.3
Case 2	614.0	514.9	451.5	359.5
Case 3	<b>600.0</b>	<b>545.5</b>	<b>475.7</b>	<b>394.6</b>

The distribution of von Mises equivalent stress in the threaded area of the horn UH1 (Fig. 8) indicates the occurrence of the maximum values on the channel between the thread turns (minor diameter), on the thread front surface and on the radius between the thread and the body of the horn. This distribution is determined by the following factors:

- Stress concentrations (the geometry of the thread was modeled according to the standardized dimensions);
- The maximum amplitude of oscillation imposed on the end surface of the horn;
- Reduced cross section of the horn in the thread area.

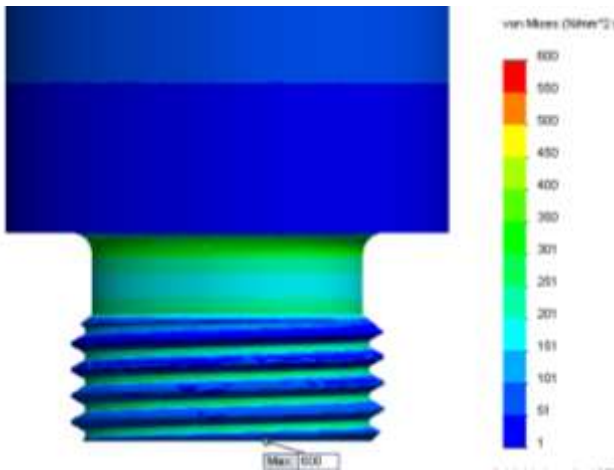


Fig. 8 Von Mises stress distribution in UH1 threaded area

The Von Mises stress distribution on the threads of UH2, UH3 and UH4 horns (Fig. 9-11) reveals a maximum value placed in the same areas as the UH1, but at lower values. The shift from the external thread M12 to the internal thread M12, lead to a reduction of the maximum stress from 600 N/mm<sup>2</sup> to 545.5 N/mm<sup>2</sup> (~ 10%). Also, by switching to the internal thread, the radius between the thread and the body of the horn is eliminated.

The decrease of the nominal size of the thread from M12 to M10 or M8 leads to a decrease of the maximum stress to 472.7 N/mm<sup>2</sup>, respectively 394.6 N/mm<sup>2</sup> (a decrease of 21% and 34% in relation to the maximum stress from the ultrasonic horn with the original geometry). During the cavitation erosion test, the specimen is not subjected to significant strains and the specimen thread size can be decreased without the occurrence of high stress.

For the analysis of the horns' fatigue behavior, the fatigue life distribution and the fatigue safety factor distribution were determined.

The minimum fatigue life was 1140785 cycles for UH1 and 5072270 cycles for UH2. The maximum values of stress for UH3 and UH4 were under the minimum alternating stress from the S-N diagram. It is considered that these geometries will not fail to fatigue. To strengthen this conclusion one must accurately know the evolution of the SN curve for 10<sup>10</sup>-10<sup>12</sup> cycles.

A more accurate assessment of fatigue behavior is obtained by analyzing the distribution of the fatigue safety factor. This was calculated as a ratio between the alternating stress from the SN diagram,  $\sigma_{SN} = 537.8 \text{ N/mm}^2$  corresponding to 10<sup>7</sup> cycles, and the equivalent stress  $\sigma_{Von Mises}$  from each node of static analysis. The limit values of the

fatigue safety factor (Table 5) indicate the possibility of using the HS3 and HS4 horns in cavitation erosion tests. Since these values are relatively small, it is recommended to impose low roughness and high geometrical precision conditions on the surface of the threaded area and on the contact front surfaces between the ultrasonic horn and the test specimen.

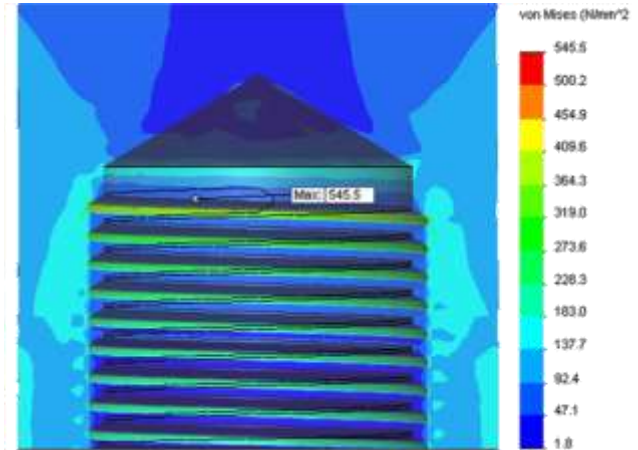


Fig. 9 Von Mises stress distribution in UH2 threaded area

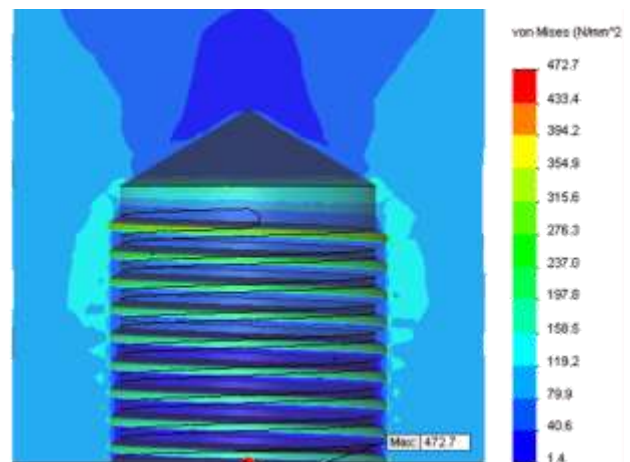


Fig. 10 Von Mises stress distribution in UH3 threaded area

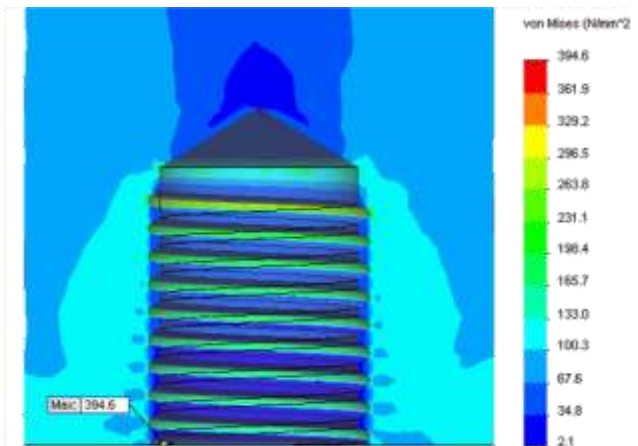


Fig. 11 Von Mises stress distribution in UH4 threaded area

Table 5  
Minimal values of fatigue factor of safety (FoS)

Horn geometry	HS1	HS2	HS3	HS4
FoS	0.897	0.986	1.131	1.363

#### 4. Conclusions

1. Static and fatigue analysis made on an ultrasonic horn used for cavitation erosion tests on vibratory systems by direct method, confirmed the conclusion resulting from experimental research: the emergence of a fatigue fracture after a number of cycles that was lower than expected for this type of components. The maximum stress occurs in the threaded area of the horn, which is designed for the attachment of the test specimen.

2. Comparing the maximum von Mises stress that occurs in the original ultrasonic horn with external thread M12 with the maximum stress that occurs on the ultrasonic horn with internal thread M12, both subject to the same constraints, it can be concluded that the internal thread generates a stress decrease of 10%. Also, the use of the internal thread removes the high stress from the radius between the thread and the body of the horn, radius used on the external thread.

3. A significant decrease of the maximum stress is generated by the decrease of the nominal size of the internal thread from M12 to M10 or M8. For the M10 and M8 threads, fatigue safety factors are above 1. The ultrasonic horn with M8 internal thread is considered to have optimal geometry in terms of fatigue behavior.

#### Acknowledgement

The work has been funded by the Sectoral Operational Programme Human Resources Development 2007-2013 of the Ministry of European Funds through the Financial Agreement POSDRU/159/1.5/S/132395.

#### References

- Bordeasu, I.** 2006. Cavitation erosion of materials, Politehnica Printing House, Timisoara, ISBN 978-973-625-278-5, 207 p.
- Standard Test Method for Cavitation Erosion Using Vibratory Apparatus. ASTM G32-10.15p.
- Hattori, S.; Ishikura, R.** 2010. Revision of cavitation erosion database and analysis of stainless steel data, *Wear* 268: 109-116.  
<http://dx.doi.org/10.1016/j.wear.2009.07.005>.
- Bregliozzi, G.; Di Schino, A.; Ahmed, S.I.-U.; Kenny, J.M.; Haefke, H.** 2005. Cavitation wear behavior of austenitic stainless steels with different grain sizes, *Wear* 258: 503-510.  
<http://dx.doi.org/10.1016/j.wear.2004.03.024>.
- Chiu, K.Y.; Cheng, F.T.; Man, H.C.** 2005. Cavitation erosion resistance of AISI 316L stainless steel laser surface-modified with NiTi, *Materials Science and Engineering A* 392: 348-358.  
<http://dx.doi.org/10.1016/j.msea.2004.09.035>.
- Cojocaru, V.; Campian, C.V.; Frunzaverde, D.; Ion, I.; Cuzmos, A.; Dumbrava, C.** 2010. Laboratory tests concerning the influence of surface hardening on the cavitation erosion resistance, *Proceedings of 3rd International Conference on Engineering Mechanics*, 210-213.
- Nedeloni, M.D.** 2012. Research regarding the cavitation erosion on materials used to manufacture the components of hydraulic turbines, PhD Thesis, "Eftimie Murgu" University, 206p. (in Romanian).
- Carboni, M.** 2014. Failure analysis of two aluminium alloy sonotrodes for ultrasonic plastic welding, *International Journal of Fatigue* 60: 110-120.  
<http://dx.doi.org/10.1016/j.ijfatigue.2013.05.013>.
- Sirbu, N.A.; Oanca, O.; Serban, S.I.** 2013. Failure analysis of the titanium alloy horn used in ultrasonic processing of polymeric materials in the automotive industry, *Metal* 2013, Brno, Czech Republic.
- Nedeloni, M.D.; Nedelcu, D.; Ion, I.; Ciubotariu, R.** 2012. Calibration of a sonotrode from a stand component for test cavitation erosion through direct method, *Constanta Maritime University's Annals* 17: 119-124.
- SolidWorks™** 2011. Material Data Library.
- Boyer, H.E.** 1986. Atlas of Fatigue Curves, ASM International, Ohio, 518p.
- Ritchie, R.O.; Davidson, D.L.; Boyce, B.L.; Campbell, J.P.; Roder, O.** 1999. High-cycle fatigue of Ti-6Al-4V, *Fatigue & Fracture of Engineering Materials & Structures* 22(7): 621-631.  
<http://dx.doi.org/10.1046/j.1460-2695.1999.00194.x>.
- Knobbe, H.; Koster, P.; Christ, A.J.; Ftitzen, C.P.; Riedler, M.** 2010. Initiation and propagation of short fatigue cracks in forged Ti6Al4V, *Procedia Engineering* 2: 931-940.  
<http://dx.doi.org/10.1016/j.proeng.2010.03.101>.
- Liu, Y.J.; Ouyang, Q.L.; Tian, R.H.; Wang, Q.Y.** 2009. Fatigue properties of Ti-6Al-4V subjected to simulated body fluid, *Structural Longevity* 2(3): 169-175.  
<http://dx.doi.org/10.3970/sl.2009.002.169>.

D. Nedelcu, V. Cojocaru, M. Nedeloni, F. Peris-Bendu, A. Ghican

#### FAILURE ANALYSIS OF A TI-6AL-4V ULTRASONIC HORN USED IN CAVITATION EROSION TESTS

#### S u m m a r y

During the testing of the materials' cavitation erosion resistance on vibratory systems by direct method (ASTM G32), the thread from the ultrasonic horn – test specimen connection, is subjected to fatigue. Operational experience has shown the occurrence of cracks and fractures in this area after a number of stress cycles that was lower than anticipated. The paper presents an analysis applied on four types of ultrasonic horns geometries: the original geometry with an external thread M12 and three modified geometries, with an internal thread M10 and M8. The four geometries were subjected to static analysis in order to determine the stress distribution. Based on static analysis, the behavior of the horns to fatigue was simulated and analyzed, determining the fatigue life, safety factors and optimal geometry.

**Keywords:** fatigue, thread, ultrasonic horn, Ti6Al4V, cavitation erosion tests.

Received February 24, 2015

Accepted July 15, 2015